Biochemical and Biophysical Research Communications 395 (2010) 471–476

Contents lists available at ScienceDirect

Biochemical and Biophysical Research Communications

journal homepage: www.elsevier.com/locate/ybbrc

Protein kinase C inhibits autophagy and phosphorylates LC3

Houbo Jiang [a], Dongmei Cheng [b,c], Wenhua Liu [a], Junmin Peng [b,c], Jian Feng [a,*]

[a] Department of Physiology and Biophysics, State University of New York at Buffalo, Buffalo, NY 14214, United States
[b] Department of Human Genetics, Center for Neurodegenerative Diseases, Emory University, Atlanta, GA 30322, United States
[c] Emory Proteomics Service Center, Emory University, Atlanta, GA 30322, United States

ARTICLE INFO

Article history:
Received 12 March 2010
Available online 14 April 2010

Keywords:
LC3
Microtubules
Autophagy
Protein kinase C
Protein phosphatase
Mass spectrometry

ABSTRACT

During autophagy, the microtubule-associated protein light chain 3 (LC3), a specific autophagic marker in mammalian cells, is processed from the cytosolic form (LC3-I) to the membrane-bound form (LC3-II). In HEK293 cells stably expressing FLAG-tagged LC3, activation of protein kinase C inhibited the autophagic processing of LC3-I to LC3-II induced by amino acid starvation or rapamycin. PKC inhibitors dramatically induced LC3 processing and autophagosome formation. Unlike autophagy induced by starvation or rapamycin, PKC inhibitor-induced autophagy was not blocked by the PI-3 kinase inhibitor wortmannin. Using orthophosphate metabolic labeling, we found that LC3 was phosphorylated in response to the PKC activator PMA or the protein phosphatase inhibitor calyculin A. Furthermore, bacterially expressed LC3 was directly phosphorylated by purified PKC *in vitro*. The sites of phosphorylation were mapped to T6 and T29 by nanoLC-coupled tandem mass spectrometry. Mutations of these residues significantly reduced LC3 phosphorylation by purified PKC *in vitro*. However, in HEK293 cells stably expressing LC3 with these sites mutated either singly or doubly to Ala, Asp or Glu, autophagy was not significantly affected, suggesting that PKC regulates autophagy through a mechanism independent of LC3 phosphorylation.

1. Introduction

Macroautophagy, referred to here as autophagy, is a dynamically regulated process for the degradation of damaged organelles, as well as aggregation-prone and long-lived proteins in cells [1,2]. The molecular basis of autophagy has been extensively studied in yeast [3]. Two ubiquitin-like conjugation systems are essential for autophagosome formation [4]. One mediates the covalent attachment of Atg12 to Atg5, and the other mediates the conjugation of Atg8 to phosphatidylethanolamine (PE). At the initiation of autophagy, Atg5–Atg12 conjugates are deposited at the Phagophore Assembly Sites (PAS). Atg5–Atg12 conjugates act in an E3-like manner to facilitate the conjugation of Atg8 to PE [5]. Atg8 is thus covalently linked to PE on the outer surface of PAS. In mammalian cells, microtubule-associated protein light chain 3 (LC3), a homologue of yeast Atg8, is the only known Atg protein associated with mature autophagosome [6]. The carboxyl terminal region of LC3 is cleaved by a cysteine protease (Atg4) to generate a soluble, cytosolic form termed as LC3-I [7]. The PE-conjugated LC3-I, known as LC3-II, covalently decorates both the inside and outside of autophagosome membranes [6]. Thus, LC3-II serves as a specific marker for autophagy in mammalian cells.

Autophagy is regulated by a number of pathways. Mammalian target of rapamycin (mTOR) is a key regulator of autophagy, although the mTOR effectors that regulate autophagy have not been identified. Phosphatidylinositol-3-kinase (PI3K), phosphatase and tension homologue (PTEN), 3-phosphoinositide-dependent protein kinase-1 (PDK1), protein kinase B (PKB), as well as tuberous sclerosis 1 and 2 (TSC1 and TSC2) are upstream regulators of the mTOR pathway [8]. Autophagy can also be induced by the product of class III PI3K, phosphatidylinositol 3-phosphate [9]. Signaling pathways mediated by eukaryotic initiation factor-2 alpha (eIF2α) kinases [10], protein kinase A (PKA) [11], Ca^{2+}/calmoduline dependent kinase II [12], and MAP kinases such as p38 and ERK [13] also regulate autophagy.

In the present study, we found that activation of protein kinase C significantly attenuated starvation- or rapamycin-induced LC3 processing. The formation of autophagosomes in response to starvation or rapamycin was blocked by PKC activators. Consistent with this, PKC inhibitors dramatically induced LC3 processing

Abbreviations: LC3, microtubule-associated protein light chain 3; PKC, protein kinase C; Bis I, bisindolylmaleimide I; IDB, thymeleatoxin, Ingenol 3, 20-dibenzoate; PMA, phorbo-12-myristate-13-acetate; CA, calyculin A; mTOR, mammalian target of rapamycin; Atg, autophagy-related gene.

* Corresponding author. Address: Department of Physiology and Biophysics, State University of New York at Buffalo, 124 Sherman Hall, Buffalo, NY 14214, United States. Fax: +1 716 829 2699.
E-mail address: jianfeng@buffalo.edu (J. Feng).

0006-291X/$ - see front matter © 2010 Elsevier Inc. All rights reserved.
doi:10.1016/j.bbrc.2010.04.030

and autophagosome formation. PKC phosphorylated LC3 both *in vivo* and *in vitro*. The sites of phosphorylation were mapped to T6 and T29 on LC3. Mutations of these residues significantly reduced LC3 phosphorylation by purified PKC *in vitro*. However, in HEK293 cells stably expressing LC3 with these sites mutated either singly or doubly to Ala, Asp or Glu, autophagy was not significantly affected, suggesting that PKC regulates autophagy through a mechanism independent of LC3 phosphorylation.

2. Materials and methods

2.1. Reagents and constructs

[γ-^{32}P]ATP (3000 Ci/mmol), [^{32}P]-orthophosphate (370 MBq/ml), ECL reagents, GSTrap™ HP columns, pGEX-4T-3 vector, and thrombin were purchased from Amersham Biosciences (Piscataway, NJ). Glutathione, 1,2-Diacyl-sn-glycero-3-phospho-L-serine, 1,2-Dioctaboyl-sn-glycero, anti-FLAG antibody, anti-FLAG-conjugated (M2) agarose, bisindolylmaleimide I (Bis I), thymeleatoxin, Ingenol 3, 20-dibenzoate (IDB), and phorbo-12-myristate-13-acetate (PMA) were from Sigma (St. Louis, MO). Wortmannin, rottlerin (Rot), rapamycin, calyculin A, Bafilomycin A1, purified rat brain protein kinase C (PKC), and purified recombinant PKC isoforms were from Calbiochem (San Diego, CA). Restriction enzymes, DNA modifying enzymes, cell culture medium and reagents, Geneticin, and isopropyl β-D-thiogalactoside were from Invitrogen (Carlsbad, CA). FuGENE 6 and protease inhibitor cocktail tablets were from Roche (Indianapolis, IN). pCMV-2A vector, QuickChange Site-Directed Mutagenesis Kit, and BL 21 *Escherichia coli* were from Stratagene (La Jolla, CA). Rat microtubule-associated protein 1 light chain 3 (LC3) was cloned by PCR amplification of rat brain cDNA with primers GCAAGCTTATGCCGTCCGAGAAGACCTTCA, which contains a Hind III site, and GCGGATCCGGATGGTCTGAGTGTCACAGTGG, which contains a BamH I site. The PCR product was sequenced and cloned into pCMV-2A, which adds a FLAG-tag at the N-terminus of LC3. LC3 cDNA was also cloned into the pGEX-4T-3, a GST fusion protein expression vector containing an N-terminal GST tag. Mutations of T6 and/or T29 of rat LC3 were performed with the QuickChange Site-Directed Mutagenesis Kit using the wild-type constructs (pCMV-2A-LC3 or pGEX-4T-3-LC3). All constructs were verified by DNA sequencing.

2.2. Purification of GST-LC3 and LC3 mutants

The pGEX-4T-3-LC3 or its mutant constructs were transformed into BL 21 *E. coli* bacterial, and fusion protein production was induced with 1 mM IPTG for 2 h at 30 °C. Cells were collected and dissolved in BugBuster protein extraction reagent (EMD Chemicals, Inc., San Diego, CA) containing protease inhibitor cocktail tablets for 20 min at room temperature. The resulting lysate was clarified by centrifugation, and fusion proteins were purified with GSTrap™ HP columns according to the manufacturer's instructions.

2.3. In vitro phosphorylation of LC3 by PKC

Recombinant GST-LC3, its mutants or histone H1 (1 μg) were incubated with 0.5 unit purified PKC or various recombinant PKC isoforms in reaction buffer containing 20 mM HEPES, pH 7.5, 10 mM $MgCl_2$, 2 mM $CaCl_2$, 100 μM ATP, 5 μCi of [γ-^{32}P]ATP, 100 μg/ml of phosphatidylserine (1,2-Diacyl-sn-glycero-3-phospho-L-serine), and 10 μg/ml of DOG(1,2-Dioctaboyl-sn-glycero) in a final volume of 50 μl. The reaction was started by the addition of [γ-^{32}P]ATP. After incubation for 15 min at 30 °C, reactions were terminated by the addition of 10 μl of 6× sample buffer and boiling for 5 min. Proteins were separated by SDS–PAGE on a 12.5% gel and transferred onto PVDF membranes. The incorporation of ^{32}P into LC3 or its mutants was visualized by autoradiograph.

2.4. In vivo phosphorylation of LC3

HEK293 cells stably expressing FLAG-LC3 or its mutants were grown in 10-cm dishes. After cells were washed six times with phosphate-free EBSS and preincubated in phosphate-free EBSS for 2 h, fresh phosphate-free EBSS containing 0.2 mCi/ml of [^{32}P]-orthophosphate was added. Thirty minutes later, 1 μM PMA were added. After incubation for 2 h at 37 °C, the cells were washed twice with ice-cold phosphate-free EBSS, and immediately lysed for 20 min on ice with cold lysis buffer containing 1% Triton X-100, 10 mM Tris–HCl, pH 7.6, 50 mM NaCl, 30 mM sodium pyrophosphate, 50 mM NaF, 5 mM EDTA, 0.1 mM Na_3VO_4 and protease inhibitors. After cell lysates were centrifuged for 30 min at 4 °C at 16,000*g*, supernatant fractions were immunoprecipitated with anti-FLAG M2-agarose affinity resin for 4 h at 4 °C. The immunoprecipitates were washed six times with ice-cold lysis buffer, separated on 12.5% SDS–PAGE, and transferred onto PVDF membrane. Autoradiograph was carried out to visualize radiolabeled proteins. After autoradiography, the membranes were blotted with anti-FLAG to verify LC3 expression.

2.5. Identification of LC3 phosphorylation sites by mass spectrometry

293/LC3 cells treated with calyculin A (100 nM for 2 h) were lysed and anti-FLAG immunoprecipitates were separated by SDS–PAGE. Coomassie blue-stained LC3-I and LC3-II bands were excised and digested in-gel with trypsin. The resulting peptides were analyzed by reverse phase liquid chromatography-tandem mass spectrometry (LC-MS/MS). GST-LC3 was phosphorylated *in vitro* by purified PKC from rat brain. After separation by SDS–PAGE and staining with Coomassie Blue G-250, the GST-LC3 band was cut from the gel and fully trypsinized as described [14]. The tryptic peptides were extracted and analyzed as previously reported [15] using an LTQ-Orbitrap hybrid mass spectrometer (Thermo Finnigan, San Jose, CA).

3. Results

3.1. Activation of protein kinase C attenuates autophagy

As LC3 is a specific marker for autophagy in mammalian cells [6], we generated HEK293 cells stably expressing N-terminal FLAG-tagged LC3 (293/LC3 cells). When these cells were treated with amino acids starvation or 50 nM rapamycin for 2 h, two well-known conditions that induce autophagy, the amount of LC3-II was dramatically increased. Wortmannin (0.5 μM), a PI-3 kinase inhibitor that blocks autophagy induced by starvation and rapamycin [16], almost completely abolished the processing of LC3 to the lipidated form, LC3-II (Supplementary Fig. 1A). These data showed that 293/LC3 cell is a valid mammalian cell model to study autophagy.

In a screen for inhibitors of autophagy, we found that activation of protein kinase C (PKC) significantly inhibited autophagy induced by starvation or rapamycin. PMA, an activator of all conventional, novel, and atypical PKC isoforms, marked attenuated the conversion of LC3-I to LC3-II by starvation or rapamycin. Thymeleatoxin (Thy), an activator of conventional PKCs and Ingenol 3, 20-dibenzoate (IDB), a more selective activator of novel PKC, also significantly blocked autophagy (Fig. 1A and B). All three PKC activators also significantly reduced the basal level of LC3-II (Fig. 1C). We found that autophagy induced by starvation or rapamycin was inhibited in a dose-dependent manner by

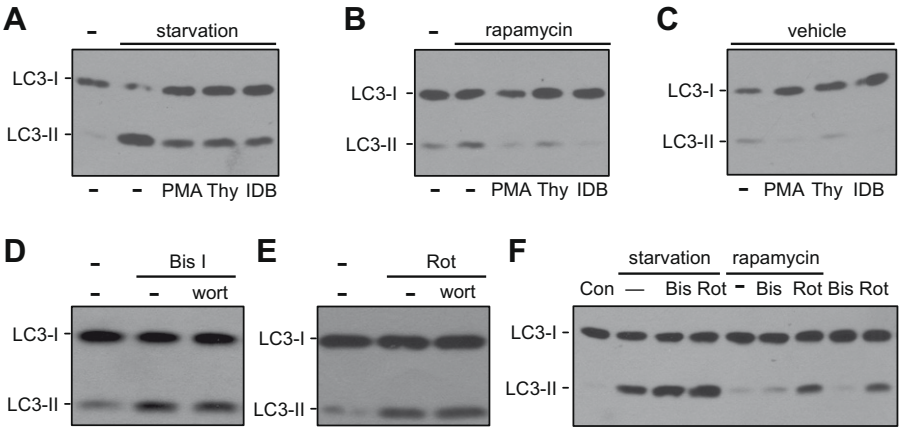

Fig. 1. Protein kinase C significantly attenuates autophagy. (A–C) 293/LC3 cells were treated with PKC activators phorbol-12-myristate-13-acetate (PMA, 1 μM), thymeleatoxin (Thy, 1 μM), or Ingenol 3, 20-dibenzoate (IDB, 1 μM) at the same time with amino acids starvation (2 h) (A) or rapamycin (50 nM for 2 h) (B) or vehicle (C). PKC activators significantly reduced the autophagic conversion of LC3-I to LC3-II that was induced by starvation (A) or rapamycin (B). Basal level of LC3 processing was also significantly decreased by these PKC activators (C). (D and E) 293/LC3 cells were treated with PKC inhibitors bisindolylmaleimide I (Bis I, 2 μM for 2 h) (D) or rottlerin (Rot, 2 μM for 2 h) (E) in the absence or presence of 0.5 μM wortmannin. PKC inhibitors markedly increased autophagy; the effect was not blocked by wortmannin. (E) 293/LC3 cells were treated with starvation or 50 nM rapamycin with or without 1.5 μM Bis I or rottlerin for 1 h. PKC inhibitors exhibited additive effects on autophagy induced by starvation or rapamycin. Con, control. All experiments were repeated at least three times with similar results.

PMA from 1 nM to 1 μM (Supplementary Fig. 2A). Consistent with these finding, various protein serine/threonine phosphatase inhibitors markedly attenuated autophagy induced by starvation or rapamycin in a dose-dependent manner (Supplementary Fig. 1B–D). Furthermore, we found that PKC inhibitors induced autophagy. The broad-spectrum PKC inhibitor bisindolylmaleimide I (Bis I) induced the autophagic conversion of LC3-I to LC3-II (Fig. 1D). Similarly, rottlerin (Rot), a potent inhibitor of PKCδ also induced autophagy (Fig. 1E). However, autophagy induced by PKC inhibitors such as Bis I or Rot was not significantly inhibited by

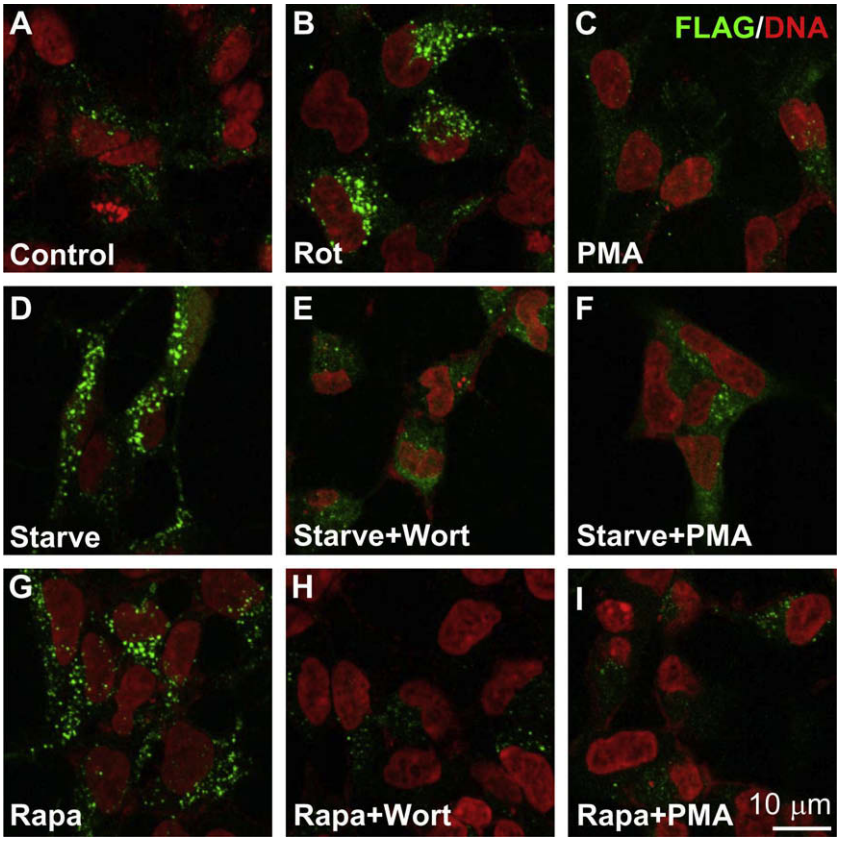

Fig. 2. The effects of PKC inhibitors and activators on the formation of autophagosomes. (A–C) 293/LC3 cells were treated without (Con, A) or with 2 μM rottlerin (Rot, B) or 1 μM PMA (C) for 2 h and co-stained for FLAG-LC3 (green) and DNA (red). Autophagosome formation was greatly increased by the PKC inhibitor rottlerin and blocked by the PKC activator PMA. (D–F) Starvation-induced increase in autophagosomes (D) was greatly blocked by wortmannin (Wort, 0.5 μM, 2 h) (E) or PMA (1 μM, 2 h) (F). (G–I) Increased formation of autophagosomes induced by rapamycin (Rapa, 50 nM, 2 h) (G) was markedly blocked by wortmannin (H) or PMA (I). Scale bar, 10 μM. The experiments were repeated at least three times with similar results. (For interpretation of color mentioned in this figure the reader is referred to the web version of the article.)

the PI-3 kinase inhibitor wortmannin (Fig. 1D and E). This is in sharp contrast to autophagy induced by starvation or rapamycin, which was potently inhibited by wortmannin (Supplementary Fig. 1A). The results suggest that autophagy induced by PKC inhibitors is not dependent on the PI-3 kinase pathway. Consistent with this, the effects of PKC inhibitors and starvation/rapamycin appeared to be additive. As shown in Fig. 1F, Bis I or Rot significantly increased the levels of LC3-II over the level induced by starvation or rapamycin. We found that both PKC inhibitors induced autophagy in a time- and dose-dependent manner (Supplementary Fig. 2B and C).

3.2. Protein kinase C regulates autophagosome formation

To confirm our findings, we used immunocytochemistry to monitor the formation of autophagosomes in 293/LC3 cells. LC3 staining showed a small amount of autophagosomes at the basal condition (Fig. 2A). After the cells were treated with the PKC inhibitor rottlerin (2 μM) for 2 h, the amount of $LC3^+$ autophagosomes greatly increased (Fig. 2B). The PKC activator PMA (1 μM for 2 h) significantly reduced the basal level of autophagosomes (Fig. 2C) and markedly attenuated autophagosome formation in response to starvation (Fig. 2, F vs. D) or rapamycin (Fig. 2, I vs. G). The efficacy of PMA appeared to be comparable to wortmannin, which inhibited autophagy induced by starvation (Fig. 2E) or rapamycin (Fig. 2H). Thus, activation of PKC blocked autophagosome formation while inhibition of PKC increased the formation of autophagosomes.

3.3. LC3 is phosphorylated in vivo on T6 in response to PMA or calyculin A

Inspection of the amino acid sequence of LC3 with NetPhos 2.0 revealed several potential PKC phosphorylation sites on LC3 [17]. To test whether LC3 is phosphorylated, we performed orthophosphate metabolic labeling assays in 293/LC3 cells. FLAG-tagged LC3 was immunoprecipitated with anti-FLAG-conjugated (M2) agarose from metabolically [^{32}P]-labeled 293/LC3 cells. [^{32}P]-phosphate incorporation into LC3 was examined by autoradiography. As shown in Fig. 3A (left panel), LC3-II phosphorylation was dramatically increased in response to the PKC activator PMA, compared to that in untreated cells. PMA-induced LC3-I phosphorylation was much less pronounced. Similarly, the protein phosphatase inhibitor calyculin A (CA) significantly increased LC3 phosphorylation, although the increase on LC3-I was more marked than that in LC3-II. Western blotting using anti-FLAG showed that the immunoprecipitates contained comparable levels of FLAG-LC3 (Fig. 3A, right panel).

To determine phosphorylation site(s) in LC3, immunoprecipitated FLAG-LC3 from 293/LC3 cells treated with CA was separated on SDS–PAGE, the FLAG-LC3 band was cut out and analyzed by trypsin digestion followed by nanoLC-coupled tandem mass spectrometry. After database search, we identified one phosphorylation site with a mass shift of 80 Da (LMPSEK$\underline{\mathbf{T}}^{6}$FR). Assignment of product ions indicated the characteristic neutral loss of phosphoric acid from the phosphopeptide during fragmentation and that the phosphorylation site was Thr6 (Fig. 3B). To further confirm the phosphorylation of Thr6 on LC3, the site was mutated to alanine and 293/LC3-T6A stable cell line was generated. As shown in Fig. 3C, phosphorylation of LC3 in response to CA or PMA was significantly decreased in 293/LC3-T6A cells compared to that in 293/LC3 cells.

3.4. LC3 is phosphorylated by PKC in vitro on T6 and T29

Next, we performed *in vitro* phosphorylation assays to investigator whether PKC directly phosphorylates LC3. GST-LC3 fusion protein expressed in *E. coli* was purified and used as a substrate

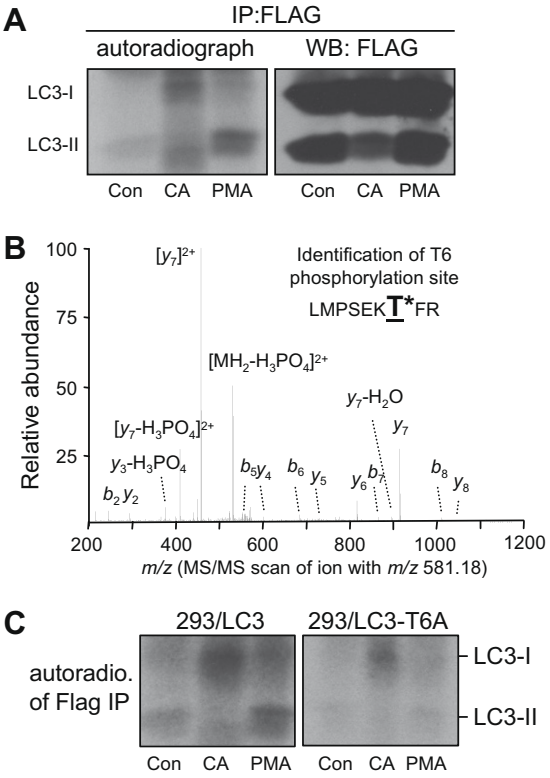

Fig. 3. LC3 is phosphorylated *in vivo* on Thr 6 site. (A) 293/LC3 cells were incubated with [^{32}P]-orthophosphate in the presence or absence of 100 nM CA or 1 μM PMA for 2 h. Cell lysates were immunoprecipitated with anti-FLAG M2-agarose and phosphorylated LC3 was visualized by autoradiography (left panel). Expression levels of LC3 were monitored by immunoblotting of the membrane with FLAG antibody after autoradiograph (right panel). (B) 293/LC3 cells were treated with 100 nM CA for 2 h. Anti-FLAG immunoprecipitates were separated by SDS–PAGE. Coomassie blue-stained LC3-I and LC3-II bands were excised and digested in-gel with trypsin. The resulting peptides were analyzed by reverse phase liquid chromatography-tandem mass spectrometry (LC-MS/MS). MS/MS scan of the precursor ion *m/z* 581.2, which was fragmented into multiple labeled product ions (*b* and *y* ions), led to the identification of a peptide with modification site on Thr 6 according to the mass shift (+80 Da) caused by phosphorylation. The neutral loss of water also occurred during the fragmentation. (C) 293/LC3 and 293/LC3-T6A cells were treated as in (A). CA- or PMA-induced phosphorylation of LC3 (left panel) was significantly decreased in LC3-T6A mutant (right panel), as shown in autoradiography of FLAG immunoprecipitates. Similar results were obtained from three independent experiments.

for purified PKC from rat brain (Calbiochem). As shown in Fig. 4A, LC3 was phosphorylated by PKC in a time-dependent manner. The bands were cut out and measured in a scintillation counter for incorporation of ^{32}P, which reached a plateau at 60 min (Fig. 4B). Thus, we used 2 h for subsequent *in vitro* phosphorylation experiments. Phosphorylation of bacterially purified GST-T6A mutant of LC3 was significantly less than the wild-type protein (Fig. 4C, left panel), suggesting that T6A is indeed phosphorylated by PKC. However, compared to histone H1, LC3 phosphorylation by PKC was rather weak (Fig. 4C, left panel). Equal loading of substrates was shown in the Coomassie blue staining of the gel (Fig. 4C, right panel), which also indicated the incomplete cleavage of the GST fusion proteins by thrombin, despite repeated trials at many conditions. The low level of LC3 phosphorylation by purified PKC from rat brain led us to examine whether certain PKC isoforms are more efficient in phosphorylating LC3. We tested various conventional (α, β_I, β_{II}, γ), novel (δ, ε, θ, η) and atypical (ι, ξ) PKC isoforms (Calbiochem) and found that most of them phosphorylated GST-LC3 to similar degree, except PKCβ_{II}, which phosphorylated GST-LC3 very weakly (Supplementary Fig. 3).

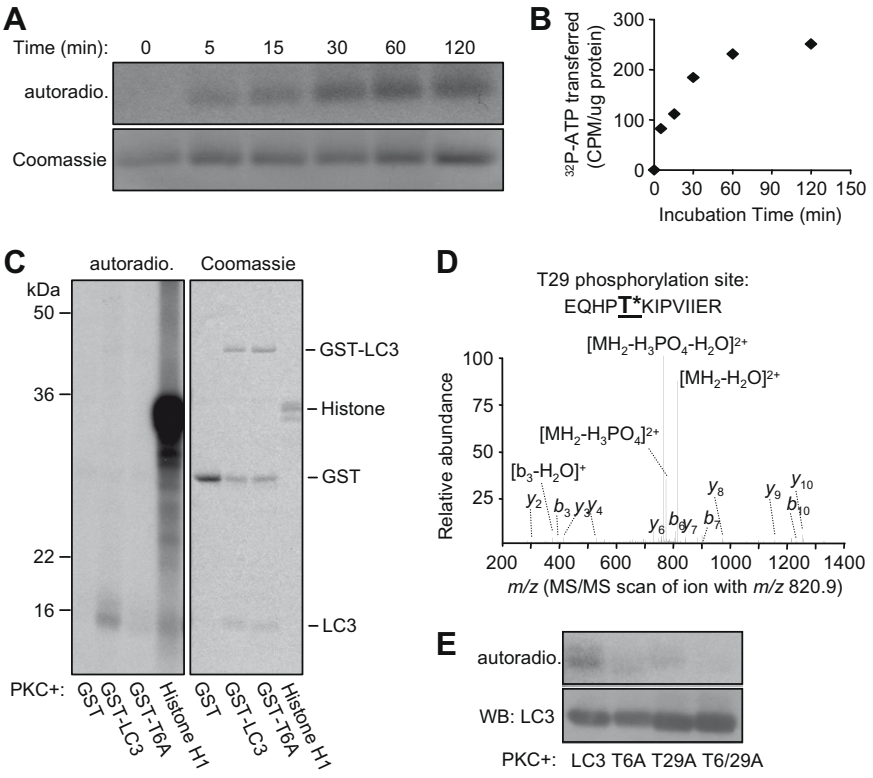

Fig. 4. LC3 is phosphorylated by PKC at T6 and T29 *in vitro*. (A and B) Phosphorylation of purified GST-LC3 by PKC *in vitro* was visualized by autoradiography (upper panel). Equal amount of GST-LC3 (1 μg) was used at each time point and the membrane was stained with Coomassie blue (lower panel) after autoradiography (A). The stained protein band was cut and [^{32}P]ATP incorporation was measured by a scintillation counter (B). (C) After GST, GST-LC3 or GST-T6A were phosphorylated *in vitro* by PKC, they were incubated with thrombin at room temperature for 2 h and separated by SDS–PAGE. Phosphorylation of LC3 and T6A were visualized by autoradiography (left panel) and the membrane was stained with Coomassie blue afterwards. Histone H1 was used as a positive control to show PKC activity. (D) After GST-LC3 was phosphorylated by PKC and separated by SDS–PAGE, the GST-LC3 band was excised and analyzed by LC-MS/MS. MS/MS scan of the precursor ion with *m/z* of 820.9 identified a peptide with phosphorylation modification on Thr 29, in addition to the previously identified phosphorylation site on Thr 6. (E) Purified GST-LC3, GST-T6A, GST-T29A and GST-T6/29A (T6A and T29A double mutant) was digested with thrombin at room temperature for 2 h and equal amounts of proteins were phosphorylated by PKC. Autoradiography showed that phosphorylation of LC3 by PKC was significantly reduced in T6A and T29A mutants and abolished in T6/29A double mutant (top panel). The membrane was blotted with anti-LC3 to show equal loading (bottom panel). Similar results were obtained from three independent experiments.

To identify PKC phosphorylation site(s) on LC3, GST-LC3 phosphorylated by PKC in the presence of non-radioactive ATP *in vitro* was analyzed by nanoLC-coupled MS/MS. Two phosphorylation sites, (LMPSEK**T**^{6}FR) and (EQHP**T**^{29}KIPVIIER) with a mass shift of 80 Da were identified (Fig. 4D). To confirm that both T6 and T29 can be phosphorylated by PKC, we generated bacterially purified GST fusion proteins of the T6A, T29A and T6A/T29A mutant LC3. *In vitro* phosphorylation of LC3 and its mutants by PKC showed that phosphorylation of LC3 was significantly reduced by T6A or T29A mutation and completely abolished by the T6A/T29A double mutations. Thus, PKC indeed can phosphorylate LC3 on T6 and T29.

To test whether LC3 phosphorylation on T6 and T29 affect autophagy, we generated stable HEK293 cell lines expressing a series of LC3 mutants. The T6A, T29A, and T6,29A mutants cannot be phosphorylated on T6, T29 or both sites, while the T6D, T29D, T6,29D, T6E, T29E, and T6,29E mutants mimic phosphorylation on either or both sites. Overexpression of these LC3 mutants did not significantly change autophagy induced by rapamycin or starvation, and did not appreciably alter the effects of PKC activators and inhibitors on autophagy (Supplementary Fig. 4).

4. Discussion

LC3 was initially identified as a microtubule-associated protein. It can bind to MAP1A and MAP1B, as well as directly to the tubulin polymer [18]. Later studies have found that LC3 plays a significant role in autophagy. In a study using GFP-LC3 transgenic mice, both LC3-I and LC3-II are shown to bind to MAP1B in the brain [19]. Overexpression of MAP1B reduces LC3-II levels and the number of autophagosomes, whereas phosphorylated MAP1B is seen on GFP-LC3^{+} autophagosomes. Together, these studies suggest that the dual functions of LC3 in binding microtubules and covalently decorating autophagosomes may be connected [20]. Our results showed that activation of PKC significantly attenuated autophagy induced by starvation or rapamycin, while inhibition of PKC markedly increased autophagy (Figs. 1 and 2). Consistent with these, protein serine/threonine phosphatases inhibitors such as calyculin A or okadaic acid markedly reduced autophagy (Supplementary Fig. 1). Because of the dual actions of LC3 in microtubule-binding and autophagy, we tested whether LC3 can be phosphorylated. Our data showed that LC3 phosphorylation in 293/FLAG-LC3 cells was significantly increased in response to PMA or calyculin A (Fig. 3A). We found that purified LC3 could be directly phosphorylated by purified PKC *in vitro* on T6 and T29 by PKC (Fig. 4). Mutations of both sites to alanine totally abolished LC3 phosphorylation by PKC *in vitro* (Fig. 4E). Thus, T6 and T29 are the major sites of phosphorylation on LC3 by PKC. The sequence context of T6 (K**T**FK) conforms to the consensus PKC phosphorylation sites (**T**/**S**XR/K), while the sequence context of T29 (P**T**KI) does not fit very well. Both sites are located in solvent-accessible positions at the N-terminal region of LC3, which belongs structurally to the ubiquitin family of proteins [21].

When we mutated T6 and T29 either individually or both to alanine, aspartic acid or glutamic acid, the autophagic conversion of LC3-I to LC3-II was not significantly affected in HEK293 cells (Supplementary Fig. 4). The simplest interpretation is that the

phosphorylation states of LC3 on T6 and T29 are not critical for autophagy; other proteins are responsible for the effects of PKC and protein phosphatase inhibitors in their regulation of autophagy. However, the presence of endogenous LC3 in HEK293 cells might have confounded this simple explanation. Because endogenous LC3 is fully capable of supporting autophagy, it appears that overexpression of LC3 phosphomutants did not exert a dominant-negative action to affect autophagy in any significantly manner. To address this possibility, it is necessary to replace endogenous LC3 with a mutant that cannot be phosphorylated by PKC. Such a knock-in experiment would be beyond the scope of the present study.

5. Conclusion

We found that activation of protein kinase C inhibited autophagy, while inhibition of protein kinase C increased autophagy. Although PKC directly phosphorylated LC3 *in vivo* and *in vitro* on T6 and T29, mutations of either or both sites do not significantly affect autophagy.

Acknowledgments

This work is supported by NIH grants NS041722, NS061856 (JF), AG025688 (JP) and NSFC grant 30928006 (JF).

Appendix A. Supplementary data

Supplementary data associated with this article can be found, in the online version, at doi:10.1016/j.bbrc.2010.04.030.

References

[1] D.J. Klionsky, Autophagy: from phenomenology to molecular understanding in less than a decade, Nat. Rev. Mol. Cell Biol. 8 (2007) 931–937.
[2] D.C. Rubinsztein, J.E. Gestwicki, L.O. Murphy, D.J. Klionsky, Potential therapeutic applications of autophagy, Nat. Rev. Drug Discov. 6 (2007) 304–312.
[3] H. Nakatogawa, K. Suzuki, Y. Kamada, Y. Ohsumi, Dynamics and diversity in autophagy mechanisms: lessons from yeast, Nat. Rev. Mol. Cell Biol. 10 (2009) 458–467.
[4] Y. Ohsumi, Molecular dissection of autophagy: two ubiquitin-like systems, Nat. Rev. Mol. Cell Biol. 2 (2001) 211–216.
[5] T. Hanada, N.N. Noda, Y. Satomi, Y. Ichimura, Y. Fujioka, T. Takao, F. Inagaki, Y. Ohsumi, The Atg12–Atg5 conjugate has a novel E3-like activity for protein lipidation in autophagy, J. Biol. Chem. 282 (2007) 37298–37302.
[6] Y. Kabeya, N. Mizushima, T. Ueno, A. Yamamoto, T. Kirisako, T. Noda, E. Kominami, Y. Ohsumi, T. Yoshimori, LC3, a mammalian homologue of yeast Apg8p, is localized in autophagosome membranes after processing, EMBO J. 19 (2000) 5720–5728.
[7] I. Tanida, Y.S. Sou, J. Ezaki, N. Minematsu-Ikeguchi, T. Ueno, E. Kominami, HsAtg4B/HsApg4B/autophagin-1 cleaves the carboxyl termini of three human Atg8 homologues and delipidates microtubule-associated protein light chain 3- and GABAA receptor-associated protein-phospholipid conjugates, J. Biol. Chem. 279 (2004) 36268–36276.
[8] S. Diaz-Troya, M.E. Perez-Perez, F.J. Florencio, J.L. Crespo, The role of TOR in autophagy regulation from yeast to plants and mammals, Autophagy 4 (2008) 851–865.
[9] A.J. Meijer, P. Codogno, Regulation and role of autophagy in mammalian cells, Int. J. Biochem. Cell Biol. 36 (2004) 2445–2462.
[10] Z. Talloczy, W. Jiang, H.W. Virgin, D.A. Leib, D. Scheuner, R.J. Kaufman, E.L. Eskelinen, B. Levine, Regulation of starvation- and virus-induced autophagy by the eIF2alpha kinase signaling pathway, Proc. Natl. Acad. Sci. USA 99 (2002) 190–195.
[11] Y.V. Budovskaya, J.S. Stephan, F. Reggiori, D.J. Klionsky, P.K. Herman, The Ras/cAMP-dependent protein kinase signaling pathway regulates an early step of the autophagy process in *Saccharomyces cerevisiae*, J. Biol. Chem. 279 (2004) 20663–20671.
[12] A. Petiot, S. Pattingre, S. Arico, D. Meley, P. Codogno, Diversity of signaling controls of macroautophagy in mammalian cells, Cell Struct. Funct. 27 (2002) 431–441.
[13] E. Ogier-Denis, S. Pattingre, J. El Benna, P. Codogno, Erk1/2-dependent phosphorylation of Galpha-interacting protein stimulates its GTPase accelerating activity and autophagy in human colon cancer cells, J. Biol. Chem. 275 (2000) 39090–39095.
[14] A. Shevchenko, M. Wilm, O. Vorm, M. Mann, Mass spectrometric sequencing of proteins silver-stained polyacrylamide gels, Anal. Chem. 68 (1996) 850–858.
[15] J. Peng, S.P. Gygi, Proteomics: the move to mixtures, J. Mass Spectrom. 36 (2001) 1083–1091.
[16] E.F. Blommaart, U. Krause, J.P. Schellens, H. Vreeling-Sindelarova, A.J. Meijer, The phosphatidylinositol 3-kinase inhibitors wortmannin and LY294002 inhibit autophagy in isolated rat hepatocytes, Eur. J. Biochem. 243 (1997) 240–246.
[17] N. Blom, S. Gammeltoft, S. Brunak, Sequence and structure-based prediction of eukaryotic protein phosphorylation sites, J. Mol. Biol. 294 (1999) 1351–1362.
[18] S.S. Mann, J.A. Hammarback, Molecular characterization of light chain 3. A microtubule binding subunit of MAP1A and MAP1B, J. Biol. Chem. 269 (1994) 11492–11497.
[19] Q.J. Wang, Y. Ding, D.S. Kohtz, N. Mizushima, I.M. Cristea, M.P. Rout, B.T. Chait, Y. Zhong, N. Heintz, Z. Yue, Induction of autophagy in axonal dystrophy and degeneration, J. Neurosci. 26 (2006) 8057–8068.
[20] Z. Yue, L. Friedman, M. Komatsu, K. Tanaka, The cellular pathways of neuronal autophagy and their implication in neurodegenerative diseases, Biochim. Biophys. Acta 1793 (2009) 1496–1507.
[21] K. Sugawara, N.N. Suzuki, Y. Fujioka, N. Mizushima, Y. Ohsumi, F. Inagaki, The crystal structure of microtubule-associated protein light chain 3, a mammalian homologue of Saccharomyces cerevisiae Atg8, Genes Cells 9 (2004) 611–618.

Supplementary Figures:

Fig. S1. Protein Serine/Threonine phosphatase inhibitors block autophagy. (A) HEK293 cells stably expressing N-terminal FLAG-tagged rat microtubule-associated protein light chain 3 (293/LC3 cells) were treated with amino acids starvation (left panel) or 50 nM rapamycin (right panel) for 2 hr in the absence or presence of 0.5 μM Wortmannin (wort). (B) 293/LC3 cells were treated with starvation or 50 nM rapamycin for 2 hr without or with the protein phosphatase inhibitor calyculin A (CA, 100 nM). (C) 293/LC3 Cells were treated with starvation or 50 nM rapamycin and CA for 2 hr at the concentrations indicated. (D) 293/LC3 cells were treated with starvation (upper panel) or 50 nM rapamycin (lower panel) for 2 hr in the absence or presence of 0.5 μM Okadaic acid (OA), 50 nM Microcystin LR, 100 nM CA, 50 μM Endothall and 10 μM FK-506. Anti-FLAG immunoblots of total cell lysates showed the processing of LC3 to LC3-I and LC3-II as indicated. Tubulin blots showed equal loading. Similar results were obtained from at least three independent experiments. Con, control.

Fig. S2. Dose response of the effects of PKC activators and inhibitors on autophagy. (A) 293/LC3 cells were treated without or with starvation (left panel) or rapamycin (50 μM, right panel) in the presence of PMA at the concentrations indicated for 2 hr. In a dose-dependent manner, PMA attenuated autophagy induced by starvation or rapamycin. (B-C) 293/LC3 cells were incubated with PKC inhibitors bisindolylmaleimide I (Bis I) or Rottlerin (Rot) at 2 μM for various durations (B) or treated for 2 h at the concentrations indicated (C). Both PKC inhibitors increased autophagy in a time- and dose-dependent manner.

Fig. S3. LC3 is phosphorylated by various PKC isoforms *in vitro*. (A) *In vitro* phosphorylation of GST-LC3 (1 μg) by various purified recombinant PKC isoforms (0.5 unit each). (B) Enzymatic activities of recombinant PKC isoforms (0.5 unit each) were monitored by the phosphorylation of histone H1 (1 μg). Con, boiled PKCα was used as control. Similar results were obtained from three independent experiments.

Fig. S4. Phosphorylation LC3 on T6 and T29 does not significantly affect autophagy. We generated HEK293 stably expressing LC3 mutants cell lines, T6A, T6D, T6E, T29A, T29D, T29E, T6A and T29A (T6A,T29A), T6D and T29D (T6D,T29D), and T6E and T29E (T6E,T29E). Cells were treated with 2.5 μM Rottlerin, 50 nM Rapamycin or starvation in the absence or presence of 1 μM PMA. Western blots of total cell lysates using antibody against FLAG. The positions of LC3-I and LC3-II are indicated. Similar results were obtained from at least three independent experiments. Con, control.

Fig. S1

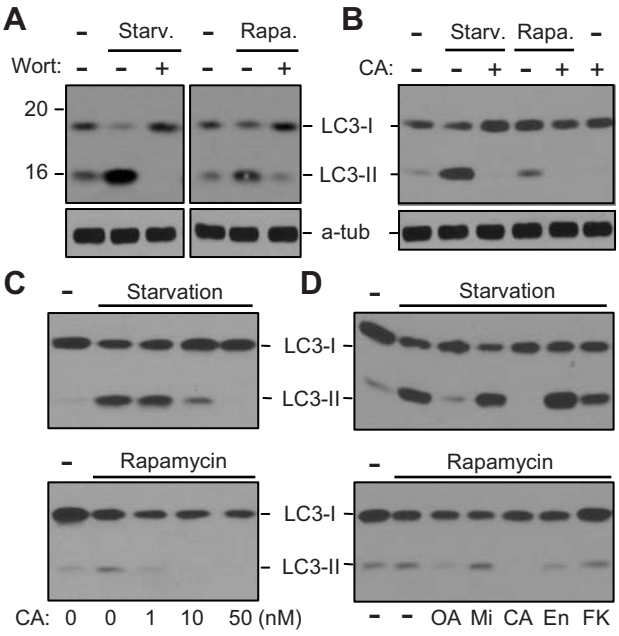
A
B
Starv.
Rapa.
Wort:
CA:
20
16
LC3-I
LC3-II
a-tub
C
D
Starvation
Rapamycin
CA: 0 0 1 10 50 (nM)
OA Mi CA En FK

Fig. S2

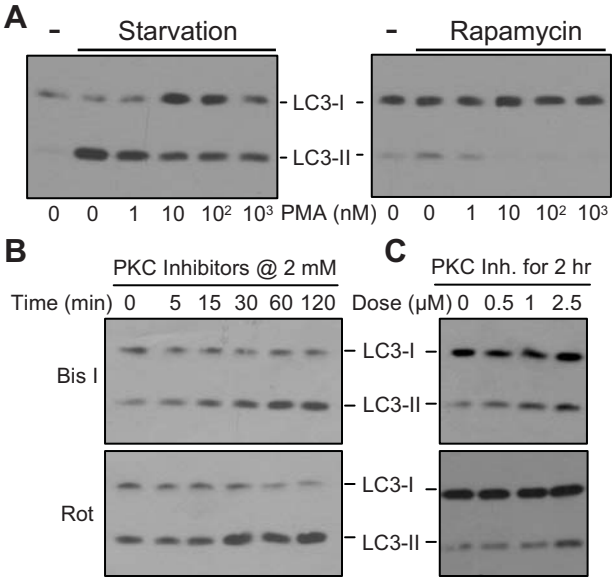
A
-
Starvation
-
Rapamycin
LC3-I
LC3-II
0 0 1 10 10² 10³ PMA (nM) 0 0 1 10 10² 10³
B
PKC Inhibitors @ 2 mM
Time (min) 0 5 15 30 60 120
Bis I
Rot
LC3-I
LC3-II
C
PKC Inh. for 2 hr
Dose (μM) 0 0.5 1 2.5

Fig. S3

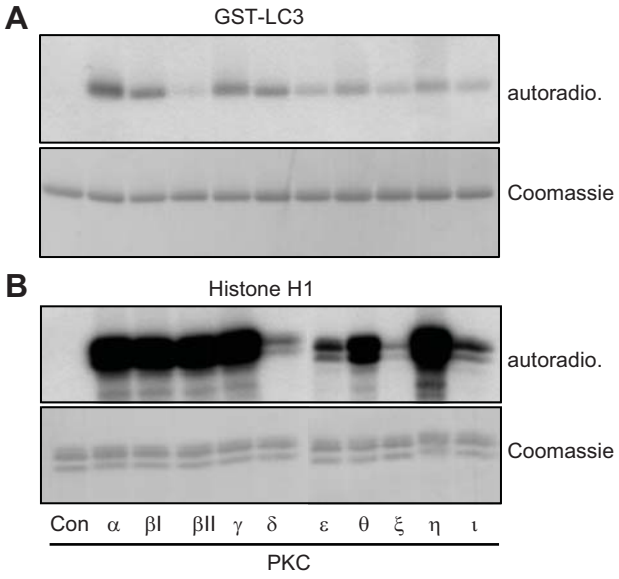
A
GST-LC3
autoradio.
Coomassie
B
Histone H1
autoradio.
Coomassie
Con α βI βII γ δ ε θ ξ η ι
PKC

Fig. S4

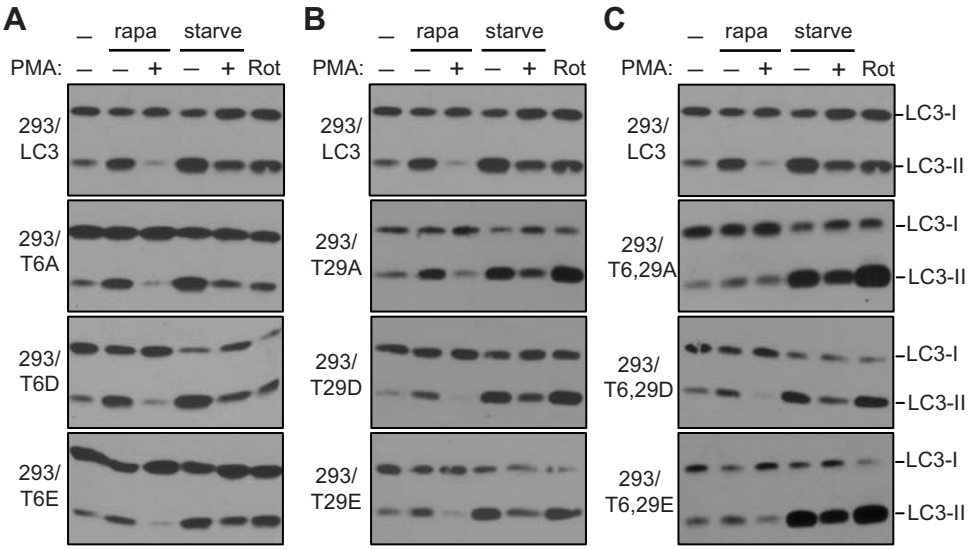
A
B
C
–
rapa
starve
PMA:
–
–
+
–
+
Rot
293/
LC3
293/
T6A
293/
T6D
293/
T6E
293/
T29A
293/
T29D
293/
T29E
293/
T6,29A
293/
T6,29D
293/
T6,29E
LC3-I
LC3-II